JOC The Journal of Organic Chemistry

pubs.acs.org/joc Article

Efficiency of Functional Group Caging with Second-Generation Green- and Red-Light-Labile BODIPY Photoremovable Protecting Groups

Pradeep Shrestha, Atreyee Mukhopadhyay, Komadhie C. Dissanayake, and Arthur H. Winter*

Cite This: J. Org. Chem. 2022, 87, 14334−14341 Read Online

ACCESS | Metrics & More | Article Recommendations | Supporting Information

ABSTRACT: BODIPY-based photocages release substrates by excitation with wavelengths in the visible to near-IR regions. The recent development of more efficient BODIPY photocages spurred us to evaluate the scope and efficiency of these second-generation boron-methylated green-light and red-light-absorbing BODIPY photocages. Here, we show that these more photosensitive photocages release amine, alcohol, phenol, phosphate, halides, and carboxylic acid derivatives with much higher quantum yields than first-generation BODIPY photocages and excellent chemical yields. Chemical yields are near-quantitative for the release of all functional groups except the photorelease of amines, which react with concomitantly photogenerated singlet oxygen. In these cases, high chemical yields for photoreleased amines are restored by irradiation under an inert atmosphere. The photorelease quantum yield has a weak relationship with the leaving group pK_a of the green-absorbing BODIPY photocages but little relationship with the red-absorbing derivatives, suggesting that factors other than leaving group quality impact the quantum yield. For the photorelease of alcohols, in all cases a carbonate linker (that loses CO_2 upon photorelease) significantly increases both the quantum yield and the chemical yield compared to those for direct photorelease via the ether.

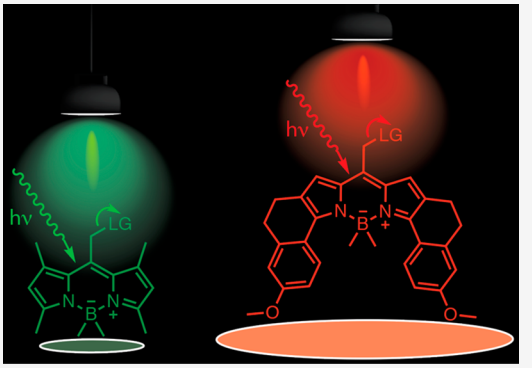

INTRODUCTION

Photocages are light-sensitive protecting groups that can be covalently linked to a biomolecule of interest to block its biological activity.[1] Upon irradiation, the covalent bond breaks and the activity of the target molecule is restored. Photocages offer spatial and temporal control over the reactivity of a substrate, making them attractive tools for investigating small molecules,[1] short-lived species,[2] therapeutic agents such as pharmaceuticals,[3,4] signaling agents,[5] neurotransmitters,[6,7] ions,[8−13] and nucleotides.[14−16] Other applications include light-responsive organic materials,[17] protecting groups in organic synthesis,[18] and the fabrication of gene chips and other microarrays.[19,20]

The most popular photocages are the *o*-nitrobenzyls[21] and their derivatives, but phenacyl,[22] acridinyl,[23] benzoinyl,[24] coumarinyl,[25,26] and *o*-hydroxynaphthyl[27] photocages also see significant use. These photocages absorb predominantly ultraviolet light, which can cause undesirable cellular photoreactions that result in cell damage or death. Photocages that absorb in the 600−1000 nm range of the electromagnetic spectrum, wavelengths in the biological window, can potentially be activated deep within living tissues with minimal phototoxicity, making them attractive for *in vivo* applications or as phototherapeutics.

Recently, BODIPY-based photocages with leaving groups substituted at the *meso*-position were developed independently by our lab and Weinstain and co-workers.[28,29] These BODIPY photocages absorb light strongly in the visible region of the optical spectrum. The first generation of green-light-absorbing BODIPY photocages featured low photorelease quantum yields, but successive iterations have significantly improved the photosensitivities, making them attractive alternatives to traditional photocages.[30] By extending the conjugation, efficient BODIPY photocages that absorb in far-red or near-IR region have been made and used in biological applications.[31,32]

However, the scope of functional groups that can be caged by the best of these BODIPY photocages has not been explored. In prior work, photocage testing was performed using a simple "dummy" carboxylic acid leaving group, typically acetic acid. Thus far, carboxylic acids, amines, alcohols, thiols, halides, xanthanes, and phenols[28−42] have been released using

Received: July 26, 2022
Published: October 18, 2022

https://doi.org/10.1021/acs.joc.2c01781
J. Org. Chem. 2022, 87, 14334−14341

BODIPY photocages. However, the evaluation of the photorelease of these functional groups was performed with the "first generation" BODIPY photocages, which are much less efficient for caging acetic acid than the most recently developed BODIPY photocages. Thus, it is currently unclear what functional groups can be released with the best of the newly developed photocages and what photorelease efficiencies and chemical yields of photorelease can be attained for the different functional groups.

Here, we explore the range of functional groups that can be photoreleased with two efficient BODIPY photocages, one BODIPY photocage that absorbs green light and one BODIPY photocage that absorbs red light. We evaluated the photorelease of alcohols, phenols, amines, phosphates, halides, and carboxylic acids. Although there appears to be some correlation between the pK_a of the protonated leaving group and the photorelease efficiency, with better leaving groups generally exhibiting higher quantum yields of photorelease, the correlation is weak and significant outliers exist, indicating that there are factors beyond leaving group quality that effect the quantum yields. Chemical yields of photorelease were nearly quantitative (>90%), making these groups potentially attractive as photoremovable protecting groups.

RESULTS AND DISCUSSION

Absorption Properties and Thermal Stability. A green-light-absorbing BODIPY (**1-PAA**; λ_{max}^{abs} = 513 nm, ε = 69 800 M^{-1} cm^{-1}) and a red-light-absorbing BODIPY (**2-AA**; λ_{max}^{abs} = 640 nm, ε = 129 000 M^{-1} cm^{-1}) were synthesized using previously developed procedures[30,43] and substituted with leaving groups (see Figure 1). Absorption spectra are shown in

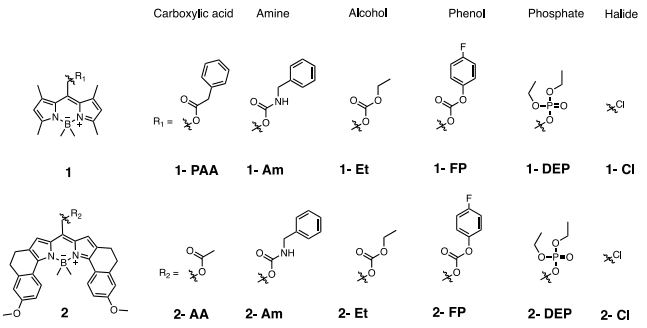

Figure 1. Second-generation green and red BODIPY compounds with different leaving groups included in this study.

Figure 2 for the esters, and the quantum yields, quantum efficiencies, and chemical photodeprotection yields are given in Table 1. The most common functional groups, including carboxylic acid, amine, alcohol, phenol, phosphate, and halide, were caged. Amines were caged via a carbamate linkage, while alcohols and phenols were caged via either an ether or a carbonate linkage. Carbonates and carbamates can undergo decarboxylation upon photorelease to generate alcohols and amines, respectively.

The thermal stabilities of all compounds were examined by keeping a solution of the photocaged substrates in the dark for 24−48 h. Photorelease quantum yield and thermal stability tests were conducted using 1:1 $CDCl_3$/MeOD as a solvent. None of the compounds in this study showed thermal release except for **1-PAA** (see the SI for details), which showed ∼20% release of phenylacetic acid over 48 h; we attribute this release

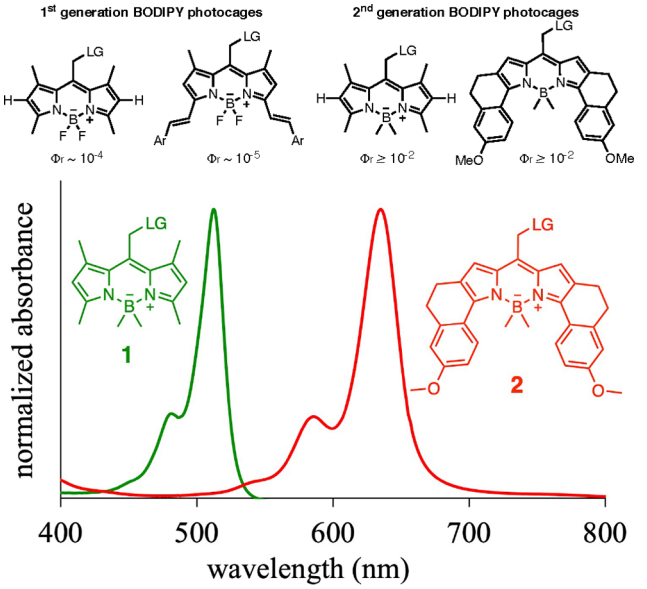

Figure 2. Normalized absorption spectra of second-generation parent ester compounds **1-PAA** and **2-AA**.

to background ester hydrolysis rather than thermal release because phenylacetic acid is a poorer ground-state leaving group than other leaving groups included in this study (e.g., Cl).

Photorelease Quantum Yields Show a Weak Relationship with Leaving Group Quality. It is a common observation that the quality of leaving groups affects the photorelease quantum yields of various photocages, particularly those believed to operate via a direct photo-S_N1 mechanism.[1] A plot of the pK_a of the protonated LG vs the quantum yield of photorelease is shown in Figure 3. For the first-generation BODIPY photocages, LGs with pK_a values considerably different from their conjugate acids, including Cl^-, AcO^-, and MeO^- (pK_a = −7.0, 4.76, and 15.5, respectively) showed a substantial difference in the photorelease quantum yield (Φ_r^{aer} = 1.62, 0.14, and 0.02%).[30,32] The second-generation BODIPY photocages described here follow a similar trend, albeit with considerably better quantum yields. The photorelease of the amine via the carbamate is an outlier to the plot of quantum yield vs pK_a for **1**. As discussed later, this outlier is attributable to a competing photodecomposition channel, where the released amine reacts with concomitantly photogenerated singlet oxygen. A sevenfold improvement in quantum yield was observed when irradiation was performed under inert atmosphere.

The variation in the quantum yields for caging different functional groups using the red derivative **2** is much narrower than that for the green BODIPY photocage **1** (Figure 3, bottom). Thus, while the plot of pK_a vs quantum yield is somewhat linear for the green-light-absorbing BODIPY **1** (particularly if the carbamate **1-Am** is excluded or if the quantum yield for **1-Am** under inert atmosphere is substituted), there is no obvious correlation with pK_a for the red-absorbing BODIPY **2**, and fluorophenol is a considerable outlier. This suggests that factors beyond leaving group quality significantly affect the photorelease quantum yields.

Photocaging of Alcohols via a Carbonate Linkage is Superior to Photocaging via Ethers. A case where the leaving group clearly matters is in photocaging of alcohols.

https://doi.org/10.1021/acs.joc.2c01781
J. Org. Chem. 2022, 87, 14334−14341

Table 1. pK_a of the Conjugate Acid of the Leaving Group, Chemical Yield of Photodeprotection, Quantum Yield of Photorelease, and Quantum Efficiency for BODIPY-Caged Compounds

	leaving group	linker	pK_a (leaving group)	chemical yield (%)	Φ_r ($\times 10^2$)[b]	$\varepsilon\Phi_r$ (M^{-1} cm^{-1})[b]
1-PAA[a]	carboxylic acid	ester	4.3	99	1.6	1100
1-Cl[a]	halide	alkyl halide	−7	100	35.0	2500
1- DEP	phosphate	phosphoester	1.4	94	35.6	25000
1-FP	phenol	carbonate	4.4	97	8.0	5700
1-Am	amine	carbamate	−1.6	55 (94)	1.0 (7.3)[d]	710
1- Et	alcohol	carbonate	4.2	96	11.6	8000
1-OBn[a]	alcohol	ether	15.5	12[c]	1.0	340
1-OPh[a]	phenol	ether	10	30[c]	1.0	510
2-AA[a]	carboxylic acid	ester	4.3	93	2.7	3800
2-Cl	halide	alkyl halide	−7	N.D	5.2	7200
2- DEP	phosphate	phosphoester	1.4	95	3.2	4400
2-FP	phenol	carbonate	4.4	93	15.2	21000
2-Am	amine	carbamate	−1.6	20 (76)[d]	1.5	2100
2- Et	alcohol	carbonate	4.2	98	3.4	4700

[a]Values reported previously.[30] [b]Photochemical efficiency $\varepsilon\Phi_r$ was calculated as the product of quantum yield (Φ_r) and the molar absorptivity at l_{max}(ε). For derivatives of both **1** and **2**, the molar extinction coefficients (ε) of the parent compounds, **1-PAA** and **2-AA**, respectively, were used by assuming that changing the leaving group did not perturb the molar absorptivity of the chromophore. All the quantum yield calculations were performed in air without purging. [c]In 20 h. [d]Under an inert atmosphere (argon). The uncaging cross-section was calculated using CD_3OD/$CDCl_3$.l_{max} = 520 and 640 nm for **1** and **2**, respectively.

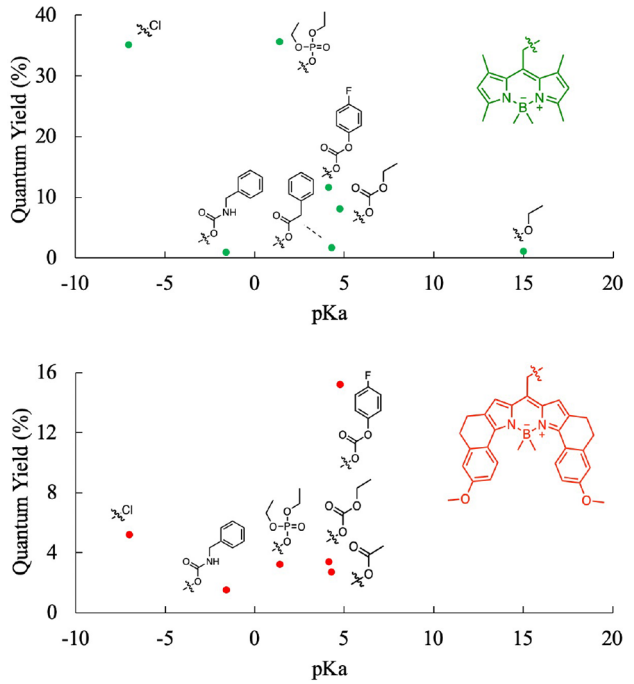

Figure 3. Plot of the pK_a of the conjugate acid of the leaving group vs quantum yield for **1** and **2**. Note that the quantum yield for photocaged benzylamine, **1-Am**, improved under an inert atmostphere to 7.3%.

There are two demonstrated ways that alcohols can be photocaged. One way is via an ether linkage,[35] and the other way is via a carbonate that eliminates CO_2 upon photorelease to generate the alcohol. In all cases, we find the carbonate linker exhibits superior photorelease efficiencies compared to the ether linkage. Chemical yields were also low when irradiation was stopped after 20 h. To study the difference in release rate with and without the carbonate linkers, we synthesized an alcohol and a phenol coupled with **1**. **1-Et** (pK_a = 4.15) has a high quantum yield of 11.6%, which is an 11-fold improvement compared to the direct release of the alcohol **1-OEt** (pK_a = 15.5) via the ether linkage. Similarly, **1-OPh** (pK_a = 4.77) has a quantum yield of 8.0%, an eightfold increase compared to structure **1-Ph** (pK_a = 10). Although caging alcohols via the ether has some advantages, including ease of synthesis and stability toward cellular esterases, the photochemical efficiencies are considerably enhanced by caging alcohols via the carbonate linkage.

However, the photorelease of amines via the related carbamate linker is surprisingly less efficient than the photorelease of alcohols via the carbonate linker. The lower quantum yield of release *and* the lower chemical yield for the release of amines suggest there are alternative photodegradation pathways. Compared to the near-quantitative chemical yields observed for caging other functional groups, the photorelease chemical yield **1-Am** is 55% and that of **2-Am** is 20%. The quantum yield for **1-Am** determined under an inert atmosphere showed a sevenfold increase compared to that determined under air irradiation(Φ_r = 7.3% vs Φ_r = 1.0%). Additionally, the chemical yield was improved from 55% under air to 94% under an inert atmosphere (argon purge). Amines are known to react with singlet oxygen to generate imines, and we determined the quantum yield by measuring product formation using ^{1}H NMR rather than by the photodecomposition of the caged compound; thus, the reaction of the released amines with $^1O_2$ diminishes the apparent quantum yield.

In conclusion, we demonstrated the release of different functional groups using second-generation green- and red-light-absorbing BODIPY photocages (**1** and **2**, respectively). The inclusion of phosphate in the list completes the tetrad of principle biomolecules, namely protein (amine and carboxylic acid), carbohydrate (alcohol), nucleic acid (phosphate), and lipid (carboxylic acid), that can be photoreleased using these photocages. The nature of the leaving group seems to play a meaningful but perhaps more muted role than anticipated in the efficiency of photorelease, particularly for the red-absorbing photocage. Perhaps this should not come as a great surprise, since the photoreaction quantum yield is an amalgam of many rate constants, not just the excited-state release rate constant.

https://doi.org/10.1021/acs.joc.2c01781
J. Org. Chem. 2022, 87, 14334−14341

Others include the rate constants for ion-pair recombination, solvent separation, internal conversion, intersystem crossing, etc. For example, for coumarin photocages, the ion-pair recombination rate is important.[44] If changing the leaving group alters any of these other rate constants in addition to the release rate constant, then a trend may not be clearly visible. Overall, however, the photochemical efficiencies of these BODIPY photocages are orders of magnitude above those of traditional UV-absorbing photocages such as *o*-nitrobenzyl and allow decaging using biologically benign green or red light. These features make BODIPY-based photocages attractive alternatives to the most popular UV-absorbing photocages.

EXPERIMENTAL SECTION

Synthesis. Amines were coupled via carbamate linkers. Intermediates **1-PNP** and **2-PNP** were obtained by reacting BODIPY alcohols with *p*-nitrobenzylchloroformate, which reacts with benzyl amine to give **1-Am** and **2-Am** (Scheme 1 and 2). To make carbonates, the BODIPY alcohol was coupled using 1,1′-carbonyldiimidazole (CDI) as a coupling agent to provide adducts **1-CDI** and **2-CDI**. Those CDI adducts react with ethanol to give **1-Et** and **2-Et**. The use of cargo as a solvent is not always a viable strategy. Hence, as a test case we reacted **2-Alc** with 2 equiv of benzyl alcohol to give **2-BA** in a 65% yield, suggesting that use of a stoichiometric quantity of a reagent is also feasible. Additionally, **1-Cl** and **2-Cl** with a halide as a leaving group were synthesized as BODIPY photocages from **1-Alc** and **2-Alc**, respectively, using a phosphorus trichloride reagent. Finally, phosphates **1-DEP** and **2-DEP** were derived from **1-Br** and **2-Cl**, respectively, by refluxing diethyl hydrogen phosphate in the presence of silver oxide.

Scheme 1. Synthesis of Second-Generation Green-Light-Absorbing BODIPY Photocages with Various Leaving Groups

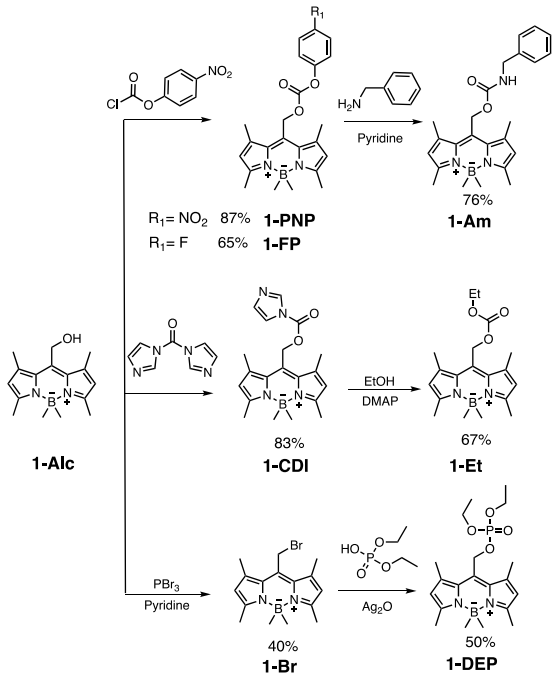

Scheme 2. Synthesis of Second-Generation Red-Light-Absorbing BODIPY Photocages with Various Leaving Groups

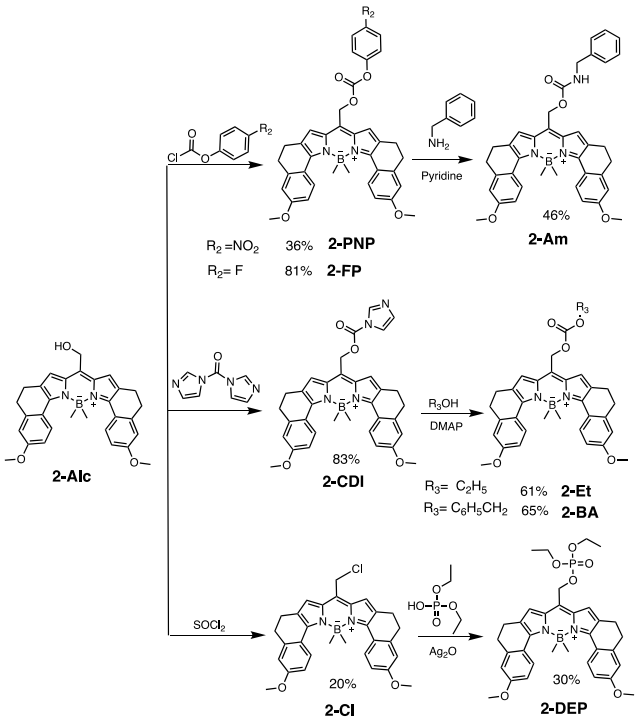

General Information. Unless stated otherwise, all puchased chemicals were used without further purification. All the reactions were carried out in the dark using the Schlenk line technique under an inert atmosphere of nitrogen. Solvents were dried using 4 Å molecular sieves. Compounds **1**, **2**, **1-Alc**, **2-Alc**, **1-Cl**, and **1-Br** were prepared as previously reported and are all known compounds;[30,32] the SI contains the procedures for their syntheses. Oil baths were used as heating sources.

Light Sources. In preliminary studies, white light was used for irradiation. An Utilitech 500 W model no. MPL 1025-C500 K9030 halogen work lamp was used as a source of white light. A 500 mL borosilicate beaker filled with water was placed between the lamp and an NMR tube as an IR cutoff filter. A fan was used to prevent the lamp from overheating. A NMR tube was placed approximately 25 cm from the light source. For the quantum yield study, a Nd:YAG laser with 532 nm emission was used as the excitation source for **1**; for **2**, a red LED from Luzchem Research Inc. was used as the excitation source.

Procedure for Determining Quantum Yields of Release. Photorelease quantum yields were determined by quantitative ^{1}H NMR spectrocopy in a 50:50 $CDCl_3$/ CD_3OD solvent using a 532 nm Nd:YAG laser or red LED (for derivatives of **2**) as a source of light. BODIPY derivatives are hydrophobic in nature; hence, an organic cosolvent was required to dissolve some of the derivatives. **1-PAA** (Φ_r = 1.6%) was used as an actinometer, and dimethyl sulfone (DMS) was used as the internal standard. Although the photodegradation quantum yield of compound **1-PAA** was reported to be 5%, quantum yield of release based on the leaving group was found to be 1.6%. The photorelease quantum yield of **1-PAA** was determined using *meso*-methyl BODIPY **1-AA** (F attached to boron and acetic acid as the LG) in CD_3OD as the actinometer. The release of the leaving group was followed using quantitative ^{1}H NMR spectroscopy (AV III 600 MHz), with a 90° pulse angle and a 20 s recycling delay cycle.

A 0.5 mM or 1 mM solution of the compound was prepared in a 1:1 mixture of deuterated methanol and deuterated chloroform. The absorbance of the solution at 532 nm was measured to ensure the absorbance was above 2 so that we could assume 100% light absorption by the sample. If the absorbance was below 2, a correction was made to allow for <100% light absorption. The sample was irradiated in a 3 mL cuvette using a 532 nm Nd:YAG laser or a Luzchem red LED. After the irradiation of the sample, 0.5 mL of the sample was transferred to an NMR tube to follow the photorelease of the leaving group via ^{1}H NMR spectroscopy (the specific signals

https://doi.org/10.1021/acs.joc.2c01781
J. Org. Chem. 2022, 87, 14334−14341

followed are depicted in the Supporting Information). The sample was then transferred back to the cuvette, and the irradiation process was continued. Dimethyl sulfone was used as the internal standard, and the release of a leaving group was determined relative to this internal standard. At least five data points were used for the calculation of the quantum yield. To ensure that the correct peak was integrated, a small amount of the leaving group was added to the solution at the end as a spike. The plot of the time in the x-axis vs the concentration of the leaving group gives a straight line, and the slope of the line provides a change in concentration per unit time. The quantum yield of release for the compounds was determined using the following equation:

$$\text{Quantum yield} = \frac{\text{Compound slope}}{\text{Actinometer slope}} \times \text{Actinometer quantum yield}$$

The determination of the quantum yield was carried out in triplicate except where noted, and the average of the three values was reported as the quantum yield of release.

For the quantum efficiencies, the molar extinction coefficients (ε) of the parent compounds **1** and **2** were used for derivatives **1-PAA** and **2-AA**, respectively, with the assumption that changing the leaving group does not perturb the molar absorptivity of the chromophore. This assumption was evaluated by determining the ε values of **1-Am** and **2-Am**, which were within 10% of those of **1-PAA** and **2-AA**, respectively.

General Procedure for Synthesis of 1-PNP, 2-PNP, 1-FP, and 2-FP. To a solution of 4-nitrophenyl or 4-fluorophenyl chloroformate (3.4 equiv) in dry CH_2Cl_2 (50 mL) was added pyridine (3.4 equiv) under a nitrogen atmosphere. The suspension was then added dropwise to a solution of compound **1-Alc** or **2-Alc** (1.04 equiv) in dry CH_2Cl_2 (100 mL) and DIPEA (4.3 equiv) at 0 °C in the dark. The reaction mixture was warmed to room temperature and stirred for 4 h. After this time, the solution was filtered through silica using CH_2Cl_2. The crude reaction mixture was washed with a 5% $NaHCO_3$ solution (2 × 50 mL), followed by water and a brine solution. The solvents were evaporated, and the product was purified by column chromatography.

1-PNP. 4-Nitrophenyl chloroformate (870 mg, 4.3 mmol, 3.4 equiv), pyridine (0.35 mL, 4.3 mmol, 3.4 equiv), **1-Alc** (280 mg, 1.036 mmol, 1 equiv), and DIPEA (0.63 mL, 4.3 mmol, 4.3 equiv) were reacted via the method reported in the general procedure. The product was purified by column chromatography using hexane/ethyl acetate (95:5) as the eluent. Compound **1-PNP** was obtained as a red solid (390 mg, 87% yield), m.p. 108−110 °C. ^{1}H NMR (600 MHz, chloroform-*d*) δ 8.31−8.27 (m, 2H), 7.43−7.38 (m, 2H), 6.12 (s, 2H), 5.61 (s, 2H), 2.48 (s,6 H), 2.46 (s, 12H), 0.20 (s, 6H). ^{13}C{1H} NMR (101 MHz, chloroform-*d*) δ 155.5, 154.0, 152.5, 145.7, 137.1, 131.3, 131.0, 125.5, 123.3, 121.8, 62.8, 16.8, 16.2. HRMS (ESI-TOF) m/z: [M + H] $^+$ calcd for $C_{23}H_{28}BN_3O_5$ 435.2080, found 435.2077.

2-PNP. 4-Nitrophenyl chloroformate (76 mg, 0.40 mmol, 3.1 equiv), pyridine (30 μL, 0.40 mmol, 3.1 equiv), **2-Alc** (60 mg, 0.13 mmol, 1 equiv), and DIPEA (46 μL, 0.40 mmol, 3.1 equiv) were reacted according to the general procedure. The product was purified by column chromatography using hexane/ethyl acetate (80:20) as the eluent. Compound **2-PNP** was obtained as a purple solid precipitate (30 mg, 36% yield), m.p. 109−111 °C. ^{1}H NMR (400 MHz, chloroform-*d*) δ 8.38−8.31 (m, 2H), 8.35−8.22 (m, 2H), 7.47−7.38 (m, 2H), 7.04−6.99 (m, 2H), 6.96−6.88 (m, 2H), 6.81 (d, J = 2.7 Hz, 2H), 5.54 (s, 2H), 3.88 (s, 6H), 2.85 (dd, J = 8.3, 5.1 Hz, 4H), 2.75 (dd, J = 8.3, 5.2 Hz, 4H), 0.59 (s, 6H). ^{13}C{^{1}H} NMR (101 MHz, chloroform-*d*) δ 160.0, 152.6, 150.6, 145.6, 143.1, 134.4, 133.1, 131.5, 127.0, 125.7, 125.5, 122.5, 122.0, 121.8, 119.1, 114.3, 111.4, 65.7, 55.5, 31.5, 29.9, 23.2. HRMS (ESI-TOF) m/z: [M] $^+$ calcd for $C_{37}H_{34}BN_3O_7$ 642.2526, found 642.2514

1-FP. 4-Fluorophenyl chloroformate (50 μL, 0.51 mmol, 3.4 equiv), pyridine (50 μL, 0.51 mmol, 3.4 equiv), **1-alc** (40 mg, 0.15 mmol, 1 equiv), and DIPEA (100 μL, 0.65 mmol, 4.3 equiv) were reacted according to the general procedure. The product was purified by column chromatography using CH_2Cl_2/ Hexane (95:5) as the eluent. Compound **1-PNP** was obtained as a red solid (40 mg, 65%), m.p. 138−142 °C. ^{1}H NMR (400 MHz, chloroform-*d*) δ 7.23−7.14 (m, 2H), 7.17−7.05 (m, 2H), 6.13 (d, J = 1.0 Hz, 2H), 5.58 (s, 2H), 2.52−2.45 (m, 12H), 0.22 (s, 6H). ^{13}C{^{1}H} NMR (101 MHz, chloroform-*d*) δ 153.8, 153.6, 137.2, 131.5, 131.4, 123.2, 122.5, 122.5, 116.5, 116.3, 62.3, 16.8, 16.2. HRMS (ESI-TOF) m/z: [M + H] $^+$ calcd for $C_{23}H_{27}BFN_2O_3$ 408.2130, found 408.2128.

2-FP. 4-Fluorophenyl chloroformate (26 μL, 0.27 mmol, 3.4 equiv), pyridine (27 μL, 0.27 mmol, 3.4 equiv), **2-alc** (40 mg, 0.08 mmol, 1 equiv), and DIPEA (55 μL, 0.34 mmol, 4.3 equiv) were reacted according to the general procedure. The product was purified by column chromatography using CH_2Cl_2/ hexanes (95:5) as the eluent. Compound **1-PNP** was obtained as a red solid (40 mg, 81% yield), m.p. 89−92 °C. ^{1}H NMR (400 MHz, chloroform-*d*) δ 8.35 (d, J = 8.9 Hz, 2H), 7.24−7.14 (m, 2H), 7.07 (dd, J = 9.2, 7.9 Hz, 2H), 7.03 (s, 2H), 6.92 (dd, J = 8.9, 2.8 Hz, 2H), 6.81 (d, J = 2.7 Hz, 2H), 5.50 (s, 2H), 3.88 (s, 6H), 2.85 (dd, J = 8.3, 5.2 Hz, 4H), 2.75 (dd, J = 8.3, 5.2 Hz, 4H), 0.60 (s, 6H). ^{13}C{^{1}H} NMR (101 MHz, chloroform-*d*) δ 160.0, 153.8, 150.4, 143.1, 134.4, 133.0, 131.5, 127.6, 122.7, 122.6, 122.6, 119.3, 116.4, 116.2, 114.2, 111.4, 65.2, 55.4, 31.5, 23.1. HRMS (ESI-TOF) m/z: [M + H] $^+$ calcd for $C_{37}H_{36}BFN_2O_5$ 616.2659, found 616.2654

General Procedure for the Synthesis of 1-Am and 2-Am. To a solution of **1-PNP or 2-PNP** (1 equiv) in dry THF (5 mL) was added a solution of pyridine in THF (1 equiv) under nitrogen gas. After stirring for 15 min at room temperature, a solution of benzylamine in THF (1.5 equiv) was added. The reaction was then stirred for an additional 3 h. Then, the solution was diluted by adding 50 mL of CH_2Cl_2 and 50 mL of water. The organic layer was washed with 1 M HCl (3 × 50 mL), 0.1 M NaOH (4 × 20 mL), and brine (50 mL). The organic layer was then dried using Na_2SO_4 and concentrated under a vacuum. The crude mixture was then purified using column chromatography (eluent solvents are given below).

1-Am. **1-PNP** (100 mg, 0.23 mmol, 1 equiv), pyridine (20 μL, 0.23 mmol, 1 equiv), and benzyl amine (45 μL, 0.35 mmol, 1.5 equiv) were reacted according to the general procedure. The crude mixture was then purified using flash chromatography using hexane/ethyl acetate (95:5) as eluent. The product was a red solid (71 mg, 76%), m.p. 171−174 °C. ^{1}H NMR (600 MHz, chloroform-*d*) δ 7.36 (m, 2H), 7.31 (m, 3H), 6.11 (s, 2H), 5.42 (s, 2H), 5.14 (t, J = 2 Hz, 1H), 4.44 (d, J = 6.0 Hz, 2H), 2.49 (s, 6H), 2.44 (s, 6H), 0.22 (s, 6H). ^{13}C{^{1}H} NMR (101 MHz, chloroform-*d*) δ 156.2, 153.3, 138.3, 137.4, 133.7, 131.3, 128.9, 127.8, 127.5, 122.8, 59.1, 45.4, 16.7, 16.1. HRMS (ESI-TOF) m/z: [M] $^+$ calcd for $C_{24}H_{31}$ BN_3O_2 403.2456, found403.2456

2-Am. **2-PNP** (30 mg, 0.05 mmol, 1 equiv), pyridine (40 μL, 0.05 mmol, 1.1 equiv), and benzylamine (75 μL, 0.08 mmol, 1.5 equiv) were reacted according to the general procedure. The crude mixture was them purified using flash chromatography using hexane/ethyl acetate (80:20) as eluent. The product was a shiny purple solid (14 mg, 46%), m.p. 132−135 °C. ^{1}H NMR (400 MHz, chloroform-*d*) δ 8.34 (d, J = 8.9 Hz, 2H), 7.31 (dq, J = 12.0, 6.4, 5.2 Hz, 5H), 7.01 (s, 2H), 6.91 (dd, J = 8.9, 2.8 Hz, 2H), 6.80 (d, J = 2.8 Hz, 2H), 5.37 (s, 2H), 5.13 (t, J = 6.1 Hz, 1H), 4.42 (d, J = 5.9 Hz, 2H), 3.87 (s, 6H), 2.83 (dd, J = 8.3, 5.3 Hz, 4H), 2.73 (dd, J = 8.4, 5.2 Hz, 4H), 0.58 (s, 6H). ^{13}C{^{1}H} NMR (101 MHz, chloroform-*d*) δ 159.8, 156.2, 150.0, 143.0, 138.3, 134.4, 132.6, 131.4, 130.0, 128.8, 127.7, 127.7, 122.7, 119.3, 114.2, 111.3, 61.6, 55.4, 45.4, 31.6, 29.8, 23.1. HRMS (ESI-TOF) m/z: [M + H]$^+$ calcd for $C_{38}H_{39}BN_3O_4$ 611.3070, found 611.3072

General Procedure for the Synthesis of 1-CDI and 2-CDI. To a solution of **1-Alc** or **2-Alc** (1 equiv) in THF (5 mL) was added CDI (2 or 10 equiv, as noted), and the reaction mixture was stirred at room temperature for 0.5 to 24 h. After the reaction was complete, 50 mL of CH_2Cl_2 was added to dilute the reaction mixture. The mixture was washed with water (2 × 50 mL), followed by brine and anhydrous Na_2SO_4. The solvent was evaporated using a rotary evaporator, and the product was purified by column chromatography in silica gel using hexanes/ethyl acetate as the eluent.

1-CDI. **1-Alc** (150 mg, 0.54 mmol, 1 equiv) and CDI (860 mg, 5.40 mmol, 10 equiv) were used, and the reaction mixture was stirred

https://doi.org/10.1021/acs.joc.2c01781
J. Org. Chem. 2022, 87, 14334−14341

overnight. The pure product was obtained from column chromatography on silica gel using hexane/ethyl acetate (80:20) as the eluent. The product was a red solid (162 mg, 83%), m.p. 123−125 °C. ^{1}H NMR (600 MHz, chloroform-*d*) δ 8.16 (s, 1H), 7.44 (s, 1H), 7.07 (s, 1H), 6.11 (s, 2H), 5.70 (s, 2H), 2.48 (s, 6H), 2.39 (s, 6H), 0.22 (s, 6H). ^{13}C{^{1}H} NMR (101 MHz, chloroform-*d*) δ 154.1, 148.6, 137.3, 137.0, 131.3, 131.1, 130.6, 123.3, 117.3, 62.0, 16.8, 16.1. HRMS (ESI-TOF) *m*/*z*: [M − H]$^-$ calcd for $C_{20}H_{24}$ BN_4O_2 362.2028, found 362.2035

2-CDI. **2-Alc** (48 mg, 0.1 mmol, 1 equiv) and CDI (33 mg, 0.2 mmol, 2 equiv) were used, and the reaction mixture was stirred at room temperature for 30 min. The product was purified by column chromatography on silica gel using hexane/ethyl acetate (2:1) as the eluent. The product was a blue solid (48 mg, 83%), m.p. 115−119 °C. ^{1}H NMR (400 MHz, chloroform-*d*) δ 8.34 (d, *J* = 8.9 Hz, 2H), 8.18 (d, *J* = 1.1 Hz, 1H), 7.46 (t, *J* = 1.5 Hz, 1H), 7.07 (dd, *J* = 1.7, 0.8 Hz, 1H), 6.99 (s, 2H), 6.92 (dd, *J* = 8.9, 2.8 Hz, 2H), 6.81 (d, *J* = 2.7 Hz, 2H), 5.63 (s, 2H), 3.87 (s, 6H), 2.85 (dd, *J* = 8.3, 5.2 Hz, 4H), 2.75 (dd, *J* = 8.5, 5.0 Hz, 4H), 0.59 (s, 6H). ^{13}C{^{1}H} NMR (101 MHz, chloroform-*d*) δ 160.0, 150.6, 148.7, 143.2, 137.5, 134.4, 133.2, 131.5, 131.0, 126.6, 122.4, 118.9, 117.5, 114.3, 111.5, 64.5, 55.4, 31.5, 23.2. HRMS (ESI-TOF) *m*/*z*: [M]$^+$ calcd for $C_{34}H_{33}BN_4O_4$ 435.2080, found 435.2077

General Procedure for the Synthesis of 1-Et, 2-Et, and 2-BA. To a solution of **1-CDI** or **2-CDI** (1 equiv) in 5 mL of ethanol or DCM was added 1 equiv of alcohol (if alcohol is not a solvent) or DMAP (1 equiv), and the reaction mixture was stirred at room temperature for 4 h. Once the reaction was complete, the reaction mixture was washed with water (3 × 50 mL) and brine and dried using Na_2SO_4. The solvent was removed on a rotary evaporator, and a clean product was obtained by column chromatography on silica gel using hexanes/ethyl acetate as the eluent.

1-Et. **1-CDI** (50 mg, 0.14 mmol, 1 equiv) in 5 mL of ethanol and DMAP (17 mg, 0.14 mmol, 1 equiv) were reacted according to the general procedure. The clean product was obtained as a brown-red solid (30 mg, 67%) by column chromatography on silica gel using hexanes/ethyl acetate (2:1) as the eluent, m.p. 126−128 °C. ^{1}H NMR (600 MHz, chloroform-*d*) δ 6.07 (s, 2H), 5.42 (s, 2H), 4.25 (q, *J* = 7.1 Hz, 2H), 2.45 (s, 6H), 2.40 (s, 6H), 1.32 (t, *J* = 7.1 Hz, 3H), 0.18 (s, 6H). ^{13}C{^{1}H} NMR (151 MHz, chloroform-*d*) δ 155.0, 153.4, 137.3, 132.3, 131.4, 122.9, 64.7, 61.4, 16.7, 16.1, 14.4. HRMS (ESI-TOF) *m*/*z*: [M + H]$^+$ calcd for $C_{19}H_{28}BN_2O_3$ 342.2229, found 342.2226.

2-Et. **2-CDI** (50 mg, 0.09 mmol, 1 equiv) in 5 mL ethanol and DMAP (10 mg, 0.09 mmol, 1 equiv) were reacted according to the general procedure. The reaction mixture was stirred at room temperature for 24 h. The clean product was obtained as a dark blue solid (30 mg, 61%) by column chromatography on silica gel using hexane/ethyl acetate (3:1) as the eluent, m.p. 113−115 °C. ^{1}H NMR (400 MHz, chloroform-*d*) δ 8.33 (d, *J* = 8.9 Hz, 2H), 7.00 (s, 2H), 6.91 (dd, *J* = 8.9, 2.8 Hz, 2H), 6.80 (d, *J* = 2.7 Hz, 2H), 5.39 (s, 2H), 4.26 (q, *J* = 7.1 Hz, 2H), 3.87 (s, 6H), 2.83 (dd, *J* = 8.3, 5.2 Hz, 4H), 2.74 (dd, *J* = 8.0, 5.4 Hz, 4H), 1.33 (t, *J* = 7.1 Hz, 3H), 0.57 (s, 6H). ^{13}C{^{1}H} NMR (151 MHz, chloroform-*d*) δ 159.8, 155.1, 150.2, 143.0, 134.4, 132.8, 131.4, 128.5, 122.6, 119.3, 114.2, 111.3, 64.7, 64.2, 55.4, 31.5, 23.1, 14.4. HRMS (ESI-TOF) *m*/*z*: [M]$^+$ calcd for $C_{33}H_{35}BN_2O_5$ [M]$^+$ 549.2675, found 549.2659

2-BA. **2-CDI** (40 mg, 0.07 mmol, 1 equiv) in 5 mL CH_2Cl_2 and DMAP (10 mg, 0.09 mmol, 1 equiv) were reacted according to the general procedure. The reaction mixture was stirred at room temperature for 24 h. The clean product was obtained as a dark blue solid (25 mg, 65%) by column chromatography on silica gel using hexanes/ethyl acetate (3:1) as the eluent, m.p. 132−135 °C. ^{1}H NMR (600 MHz, chloroform-*d*) δ 8.34 (d, *J* = 8.9 Hz, 2H), 7.42−7.27 (m, 8H), 6.99 (s, 2H), 6.91 (dd, *J* = 8.9, 2.8 Hz, 2H), 6.80 (d, *J* = 2.7 Hz, 2H), 5.40 (d, *J* = 9.9 Hz, 2H), 5.22 (s, 2H), 3.87 (s, 6H), 2.83 (dd, *J* = 8.4, 5.5 Hz, 4H), 2.73 (dd, *J* = 8.1, 5.8 Hz, 4H), 0.57 (s, 6H). ^{13}C{^{1}H} NMR (151 MHz, chloroform-*d*) δ 159.8, 150.2, 143.0, 135.1, 134.4, 132.8, 131.4, 128.8, 128.7, 128.7, 128.6, 127.8, 127.1, 122.6, 119.3, 114.2, 111.3, 70.3, 64.5, 55.4, 31.5, 23.1. HRMS (ESI-TOF) *m*/*z*: [M]$^+$ calcd for $C_{38}H_{37}BN_2O_5$ 611.2832, found 611.2813

2-Cl. To the solution of **2-Alc** (100 mg, 0.2 mmol, 1 equiv) in 10 mL of dry toluene were added a few drops of DMF. To the reaction mixture was added thionyl chloride (15 μL, 0.2 mmol, 1 equiv), and the mixture was stirred for 10 min. After the completion of the reaction, it was quenched with water (10 mL). The reaction mixture was washed with a saturated sodium bicarbonate solution and brine and dried using Na_2SO_4. The solvent was removed on a rotary evaporator, and a pure product was obtained as a blue solid (20 mg, 20%) by flash chromatography in silica gel using CH_2Cl_2/hexanes (1:4) as the eluent, m.p. 226−228 °C. ^{1}H NMR (400 MHz, chloroform-*d*) δ 8.32 (d, *J* = 8.9 Hz, 2H), 6.97 (s, 2H), 6.91 (dd, *J* = 8.8, 2.8 Hz, 2H), 6.80 (d, *J* = 2.7 Hz, 2H), 4.77 (s, 2H), 3.87 (s, 6H), 2.85 (dd, *J* = 8.2, 5.3 Hz, 4H), 2.75 (dd, *J* = 8.3, 5.2 Hz, 4H), 0.57 (s, 6H). ^{13}C{^{1}H} NMR (101 MHz, chloroform-*d*) δ 159.9, 150.1, 143.0, 133.6, 132.9, 131.4, 131.21, 122.6, 118.4, 114.2, 111.4, 55.4, 40.0, 31.5, 29.8, 23.2. HRMS (ESI-TOF) *m*/*z*: [M]$^+$ calcd for $C_{30}H_{30}BClN_2O_2$ 495.2125, found 495.2116

General Procedure for the Synthesis of 1-DEP or 2-DEP. To a solution of **1-Br** or **2-Cl** (1 equiv) in 3 mL of dry acetonitrile were added diethyl phosphate (2−5 equiv) and silver oxide (2−5 equiv). The reaction mixture was refluxed at 80 °C for 10 h. After the reaction was complete, the insoluble silver oxide was removed by filtration, and the crude reaction mixture was washed with water followed by a saturated ammonium chloride solution and brine and dried using anhydrous Na_2SO_4. The solvent was removed on a rotary evaporator, and the pure product was obtained by flash chromatography on silica gel using hexanes/ethyl acetate (50:50) as the eluent.

1-DEP. **1-Br** (40 mg, 0.10 mmol, 1 equiv), diethyl phosphate (35 μL, 0.20 mmol, 2 equiv), and silver oxide (50 mg, 0.22 mmol, 2 equiv) were reacted according to the general procedure. The product obtained was a red solid (20 mg, 50%), m.p. 103−106 °C. ^{1}H NMR (400 MHz, chloroform-*d*) δ 6.08 (s, 2H), 5.39 (d, *J* = 5.2 Hz, 2H), 4.11 (p, *J* = 7.2 Hz, 4H), 2.52 (s, 6H), 2.45 (s, 6H), 1.29 (td, *J* = 7.1, 1.1 Hz, 7H), 0.18 (s, 6H). ^{13}C{^{1}H} NMR (101 MHz, chloroform-*d*) δ 153.5, 137.7, 133.6, 133.5, 131.1, 123.0, 64.3, 64.3, 60.4, 60.4, 16.8, 16.2, 16.2, 16.2. ^{31}P{^{1}H} NMR (162 MHz, chloroform-*d*) δ −1.34. HRMS (ESI-TOF) *m*/*z*: [M + H]$^+$ calcd for $C_{20}H_{333}BN_2O_4P$ 406.2307, found 406.2292

2-DEP. **2-Cl** (20 mg, 0.04 mmol, 1 equiv), diethyl phosphate (35 μL, 0.20 mmol, 5 equiv), and silver oxide (50 mg, 0.22 mmol, 5 equiv) were reacted according to the general procedure. The product was a blue solid (7 mg, 30%). ^{1}H NMR (400 MHz, chloroform-*d*) δ 8.33 (d, *J* = 8.9 Hz, 2H), 7.05 (s, 2H), 6.91 (dd, *J* = 8.9, 2.8 Hz, 2H), 6.80 (d, *J* = 2.8 Hz, 2H), 5.26 (d, *J* = 8.8 Hz, 2H), 4.17−4.03 (m, 4H), 3.87 (s, 6H), 2.83 (dd, *J* = 8.2, 5.1 Hz, 4H), 2.74 (dd, *J* = 8.1, 5.4 Hz, 4H), 1.37−1.23 (m, 6H), 0.56 (s, 6H). ^{13}C{^{1}H} NMR (101 MHz, chloroform-*d*) δ 159.8, 150.2, 143.0, 134.2, 132., 131.4, 122.6, 119.3, 114.2, 111.3, 64.3, 64.2, 63.9, 55.4, 31.6, 29.8, 23.1, 16.3, 16.2, 1.2. ^{31}P{^{1}H} NMR (162 MHz, chloroform-*d*) δ −1.10. HRMS (ESI-TOF) *m*/*z*: [M]$^+$ calcd for $C_{34}H_{40}BN_2O_6$ was 613.2753, found 613.2752

■ ASSOCIATED CONTENT

Supporting Information

The Supporting Information is available free of charge at https://pubs.acs.org/doi/10.1021/acs.joc.2c01781.

Procedures for the synthesis of previously reported compounds; ^{1}H NMR spectra of the preliminary tests; and characterization of the newly synthesized compounds, including ^{1}H NMR, ^{13} C{^{1}H}, and HRMS spectra (PDF)

https://doi.org/10.1021/acs.joc.2c01781
J. Org. Chem. 2022, 87, 14334−14341

AUTHOR INFORMATION

Corresponding Author

Arthur H. Winter − *Department of Chemistry, Iowa State University, Iowa 50010, United States;* orcid.org/0000-0003-2421-5578; Email: winter@iastate.edu

Authors

Pradeep Shrestha − *Department of Chemistry, Iowa State University, Iowa 50010, United States;* orcid.org/0000-0003-4166-966X

Atreyee Mukhopadhyay − *Department of Chemistry, Iowa State University, Iowa 50010, United States*

Komadhie C. Dissanayake − *Department of Chemistry, Iowa State University, Iowa 50010, United States;* orcid.org/0000-0003-3347-1004

Complete contact information is available at: https://pubs.acs.org/10.1021/acs.joc.2c01781

Notes

The authors declare no competing financial interest.

ACKNOWLEDGMENTS

We thank the PRF 62317-ND4 and the National Science Foundation for supporting this work through CHE-2055335.

REFERENCES

(1) Klan, P.; Solomek, T.; Bochet, C. G.; Blanc, A.; Givens, R.; Rubina, M.; Popik, V.; Kostikov, A.; Wirz, J. Photoremovable Protecting Groups in Chemistry and Biology: Reaction Mechanisms and Efficacy. *Chem. Rev.* **2013**, *113*, 119.

(2) Li, M.-D.; Wong, N.-K.; Xiao, J.; Zhu, R.; Wu, L.; Dai, S.-Y.; Chen, F.; Huang, G.; Xu, L.; Bai, X.; Geraskina, M. R.; Winter, A. H.; Chen, X.; Liu, Y.; Fang, W.; Yang, D.; Phillips, D. L. Dynamics of Oxygen-Independent Photocleavage of Blebbistatin as a One-Photon Blue or Two-Photon Near-Infrared Light-Gated Hydroxyl Radical Photocage. *J. Am. Chem. Soc.* **2018**, *140* (46), 15957−15968.

(3) Lin, Q.; Huang, Q.; Li, C.; Bao, C.; Liu, Z.; Li, F.; Zhu, L. Anticancer Drug Release from a Mesoporous Silica Based Nano-photocage Regulated by either a one- or two-photon process. *J. Am. Chem. Soc.* **2010**, *132* (31), 10645.

(4) Liu, M.; Meng, J.; Bao, W.; Liu, S.; Wei, W.; Ma, G.; Tian, Z. Single-Chromophore-Based Therapeutic Agent Enables Green-Light-Triggered Chemotherapy and Simultaneous Photodynamic Therapy to Cancer Cells. *ACS Applied Bio Materials* **2019**, *2* (7), 3068−3076.

(5) Mayer, G.; Heckel, A. Biologically Active Molecules with a "Light Switch". *Angew. Chem., Int. Ed* **2006**, *45* (30), 4900−4921.

(6) Adams, S. R.; Tsien, R. Y. Controlling cell chemistry with caged compounds. *Annu. Rev. Physiol.* **1993**, *55*, 755.

(7) Ellis-Davies, G. C. R. Caged compounds: photorelease technology for control of cellular chemistry and physiology. *Nat. Methods* **2007**, *4* (8), 619.

(8) Mbatia, H. W.; Bandara, H. M. D.; Burdette, S. C. CuproCeav-1, a first generation photocage for Cu^{+}. *Chem. Commun.* **2012**, *48*, 5331−5333.

(9) Atilgan, A.; Çeçik, E. T.; Guliyev, R.; Uyar, T. B.; Erbas-Cakmak, S.; Akkaya, E. U. Near-IR-Triggered, Remote-Controlled Release of Metal Ions: A Novel Strategy for Caged Ions. *Angew. Chem., Int. Ed.* **2014**, *53* (40), 10678−10681.

(10) Kaplan, J. H.; Ellis-Davies, G. C. Photolabile chelators for the rapid photorelease of divalent cations. *Proc. Natl. Acad. Sci. U.S.A.* **1988**, *85* (17), 6571.

(11) Gomez, T. M.; Spitzer, N. C. In vivo regulation of axon extension and pathfinding by growth-cone calcium transients. *Nature* **1999**, *397* (6717), 350−355.

(12) Brown, E. B.; Shear, J. B.; Adams, S. R.; Tsien, R. Y.; Webb, W. W. Photolysis of caged calcium in femtoliter volumes using two-photon excitation. *Biophys. J.* **1999**, *76*, 489.

(13) Kramer, R. H.; Chambers, J. J.; Trauner, D. Photochemical tools for remote control of ion channels in excitable cells. *Nat. Chem. Biol.* **2005**, *1* (7), 360.

(14) Kaplan, J. H.; Forbush, B.; Hoffman, J. F. Rapid photolytic release of adenosine 5′-triphosphate from a protected analog: utilization by the sodium:potassium pump of human red blood cell ghosts. *Biochemistry* **1978**, *17* (10), 1929−1935.

(15) Walbert, S.; Pfleiderer, W.; Steiner, U. E. Photolabile Protecting Groups for Nucleosides: Mechanistic Studies of the 2-(2-Nitrophenyl)ethyl Group. *Helv. Chim. Acta* **2001**, *84* (6), 1601−1611.

(16) Walker, J. W.; Reid, G. P.; McCray, J. A.; Trentham, D. R. Photolabile 1-(2-nitrophenyl)ethyl phosphate esters of adenine nucleotide analogs. Synthesis and mechanism of photolysis. *J. Am. Chem. Soc.* **1988**, *110* (21), 7170−7177.

(17) Katz, J. S.; Burdick, J. A. Light-Responsive Biomaterials: Development and Applications. *Macromol. Biosci.* **2010**, *10*, 339.

(18) (i) Wuts, P. G. M.; Greene, T. W.*Greene's Protective Groups in Organic Synthesis*, 4th ed.; Wiley, 2006. (ii) Leichnitz, S.; Dissanayake, K.; Winter, A. H.; Seeberger, P. Photolabile BODIPY Protecting Groups for Glycan Synthesis. *Chem. Commun.* **2022**, *58*, 10556. (iii) Peterson, J.; Yuan, D.; Winter, A. H. Multiwavelength Control of Mixtures Using Visible Light-Absorbing Photocages. *J. Org. Chem.* **2021**, *86* (14), 9781−9787.

(19) Pirrung, M. C. Spatially Addressable Combinatorial Libraries. *Chem. Rev.* **1997**, *97*, 473.

(20) Kretschy, N.; Holik, A. K.; Somoza, V.; Stengele, G. P.; Somoza, M. M. Next-Generation o-Nitrobenzyl Photolabile Groups for Light-Directed Chemistry and Microarray Synthesis. *Angew. Chem., Int. Ed.* **2015**, *54*, 8555.

(21) *Dynamic Studies in Biology: Phototriggers, Photoswitches and Caged Biomolecules*; Goeldner, M., Givens, R., Eds.; Wiley, 2006.

(22) Park, C. H.; Givens, R. S. New Photoactivated Protecting Groups. 6. p-Hydroxyphenacyl: A Phototrigger for Chemical and Biochemical Probes. *J. Am. Chem. Soc.* **1997**, *119* (10), 2453.

(23) Ackmann, A. J.; Frechet, M. J. The generation of hydroxide and methoxide ions by photo-irradiation: use of aromatization to stabilize ionic photo-products from acridine derivatives. *Chem. Commun.* **1996**, *5*, 605.

(24) Sheehan, J. C.; Wilson, R. M.; Oxford, A. W. Photolysis of methoxy-substituted benzoin esters. Photosensitive protecting group for carboxylic acids. *J. Am. Chem. Soc.* **1971**, *93* (26), 7222−7228.

(25) Givens, R. S.; Matuszewski, B. Photochemistry of phosphate esters: an efficient method for the generation of electrophiles. *J. Am. Chem. Soc.* **1984**, *106* (22), 6860−6861.

(26) Olson, J. P.; Banghart, M. R.; Sabatini, B. L.; Ellis-Davies, G. C. R. Spectral Evolution of a Photochemical Protecting Group for Orthogonal Two-Color Uncaging with Visible Light. *J. Am. Chem. Soc.* **2013**, *135* (42), 15948−15954.

(27) Arumugam, S.; Popik, V. V. Photochemical generation and the reactivity of o-naphthoquinone methides in aqueous solutions. *J. Am. Chem. Soc.* **2009**, *131* (33), 11892.

(28) Goswami, P.; Syed, A.; Beck, C. L.; Albright, T. R.; Mahoney, K. M.; Unash, R.; Smith, E. A.; Winter, A. H. BODIPY-Derived Photoremovable Protecting Groups Unmasked with Green Light. *J. Am. Chem. Soc.* **2015**, *137*, 3783.

(29) Rubinstein, N.; Liu, P.; Miller, E. W.; Weinstain, R. meso-Methylhydroxy BODIPY: a scaffold for photo-labile protecting groups. *Chem. Commun.* **2015**, *51*, 6369.

(30) Slanina, T.; Shrestha, P.; Palao, E.; Kand, D.; Peterson, J. A.; Dutton, A. S.; Rubinstein, N.; Weinstain, R.; Winter, A. H.; Klan, P. In Search of the Perfect Photocage: Structure Reactivity Relationships in meso-Methyl BODIPY Photoremovable Protecting Groups. *J. Am. Chem. Soc.* **2017**, *139* (42), 15168−15175.

(31) Peterson, J. A.; Wijesooriya, C.; Gehrmann, E. J.; Mahoney, K. M.; Goswami, P. P.; Albright, T. R.; Syed, A.; Dutton, A. S.; Smith, E. A.; Winter, A. H. Family of BODIPY Photocages Cleaved by Single

Photons of Visible/Near-Infrared Light. *J. Am. Chem. Soc.* **2018**, *140* (23), 7343−7346.
(32) Shrestha, P.; Dissanayake, K. C.; Gehrmann, E. J.; Wijesooriya, C. S.; Mukhopadhyay, A.; Smith, E. A.; Winter, A. H. Efficient Far-Red/Near-IR Absorbing BODIPY Photocages by Blocking Unproductive Conical Intersections. *J. Am. Chem. Soc.* **2020**, *142* (36), 15505−15512.
(33) Sitkowska, K.; Feringa, B. L.; Szymański, W. Green-Light-Sensitive BODIPY Photoprotecting Groups for Amines. *J. Org. Chem.* **2018**, *83* (4), 1819.
(34) Sitkowska, K.; Hoes, M. F.; Lerch, M. M.; Lameijer, L. N.; van der Meer, P.; Szymański, W.; Feringa, B. L. Red-light-sensitive BODIPY photoprotecting groups for amines and their biological application in controlling heart rhythm. *Chem. Commun.* **2020**, *56* (41), 5480−5483.
(35) Peterson, J. A.; Fischer, L. J.; Gehrmann, E. J.; Shrestha, P.; Yuan, D.; Wijesooriya, C. S.; Smith, E. A.; Winter, A. H. Direct Photorelease of Alcohols from Boron-Alkylated BODIPY Photocages. *J. Org. Chem.* **2020**, *85* (8), 5712−5717.
(36) Toupin, N. P.; Arora, K.; Shrestha, P.; Peterson, J. A.; Fischer, L. J.; Rajagurubandara, E.; Podgorski, I.; Winter, A. H.; Kodanko, J. J. BODIPY-Caged Photoactivated Inhibitors of Cathepsin B Flip the Light Switch on Cancer Cell Apoptosis. *ACS Chem. Biol.* **2019**, *14* (12), 2833−2840.
(37) Štacko, P.; Muchová, L.; Vítek, L.; Klán, P. Visible to NIR Light Photoactivation of Hydrogen Sulfide for Biological Targeting. *Org. Lett.* **2018**, *20* (16), 4907−4911.
(38) Blangetti, M.; Fraix, A.; Lazzarato, L.; Marini, E.; Rolando, B.; Sodano, F.; Fruttero, R.; Gasco, A.; Sortino, S. A Nonmetal-Containing Nitric Oxide Donor Activated with Single-Photon Green Light. *Chemistry* **2017**, *23* (38), 9026−9029.
(39) Dockalova, V.; Sanchez-Carnerero, E. M.; Dunajova, Z.; Palao, E.; Slanska, M.; Buryska, T.; Damborsky, J.; Klán, P.; Prokop, Z. Fluorescent substrates for haloalkane dehalogenases: Novel probes for mechanistic studies and protein labeling. *Comput. Struct Biotechnol J.* **2020**, *18*, 922−932.
(40) Faggi, E.; Aguilera, J.; Sáez, R. n.; Pujol, F.; Marquet, J.; Hernando, J.; Sebastián, R. M. a. Wavelength-Tunable Light-Induced Polymerization of Cyanoacrylates Using Photogenerated Amines. *Macromolecules* **2019**, *52* (6), 2329−2339.
(41) Vohradská, N.; Sánchez-Carnerero, E. M.; Pastierik, T.; Mazal, C.; Klán, P. Controlled photorelease of alkynoic acids and their decarboxylative deprotection for copper-catalyzed azide/alkyne cycloaddition. *Chem. Commun.* **2018**, *54* (44), 5558−5561.
(42) Li, M.; Dove, A. P.; Truong, V. X. Additive-Free Green Light-Induced Ligation Using BODIPY Triggers. *Angew. Chem., Int. Ed.* **2020**, *59* (6), 2284−2288.
(43) Antony, L. A. P.; Slanina, T.; Sebej, P.; Solomek, T.; Klan, P. Fluorescein Analogue Xanthene-9-Carboxylic Acid: A Transition-Metal-Free CO Releasing Molecule Activated by Green Light. *Org. Lett.* **2013**, *15* (17), 4552.
(44) (i) Schmidt, R.; Geissler, D.; Hagen, V.; Bendig, J. Kinetics Study of the Photocleavage of (Coumarin-4-yl)methyl Esters. *J. Phys. Chem. A* **2005**, *109* (23), 5000−5004. (ii) Schmidt, R.; Geissler, D.; Hagen, V.; Bendig. Mechanism of Photocleavage of (Coumarin-4-yl)methyl Esters. *J. Phys. Chem. A* **2007**, *111*, 5768−5774. (iii) Schulte, A.; Alachouzos, G.; Szymanski, W.; Feringa, B. Strategy for Engineering High Photolysis Efficiency of Photocleavable Protecting Groups through Cation Stabilization. *J. Am. Chem. Soc.* **2022**, *144* (27), 12421−12430.

https://doi.org/10.1021/acs.joc.2c01781
J. Org. Chem. 2022, 87, 14334−14341